Supplemental Material

Structural basis for norovirus inhibition and fucose mimicry by citrate

Grant S. Hansman, Syed Shahzad-ul-Hussan, Jason S. McLellan, Gwo-Yu Chuang, Ivelin Georgiev, Takashi Shimoike, Kazuhiko Katayama, Carole A. Bewley, and Peter D. Kwong

Table of Contents

Figure S1

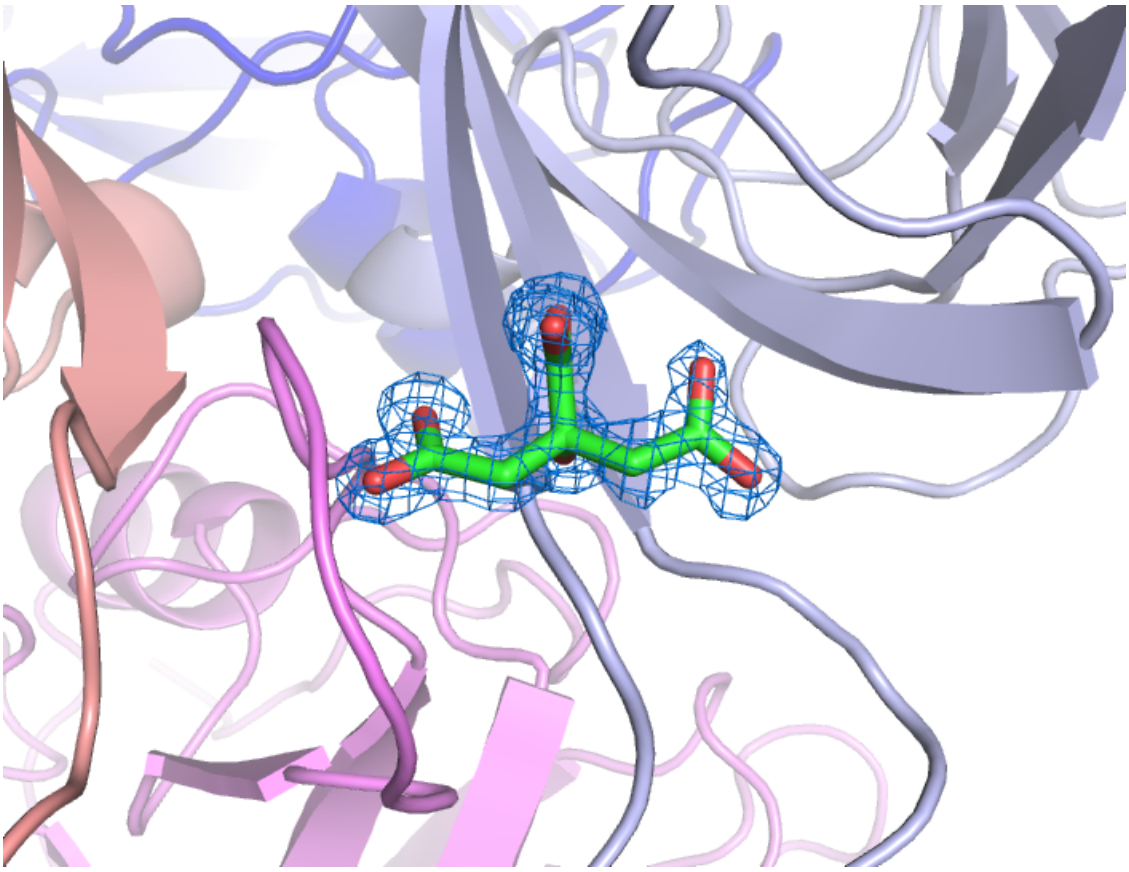

Figure S1. The citrate density was verified using a simulated-annealing $2F_o$-F_c OMIT map. The GII.10 P domain was colored as in Fig. 1A, the citrate was colored green, and the electron density (blue mesh) was contoured at 1.0 sigma.

Figure S2

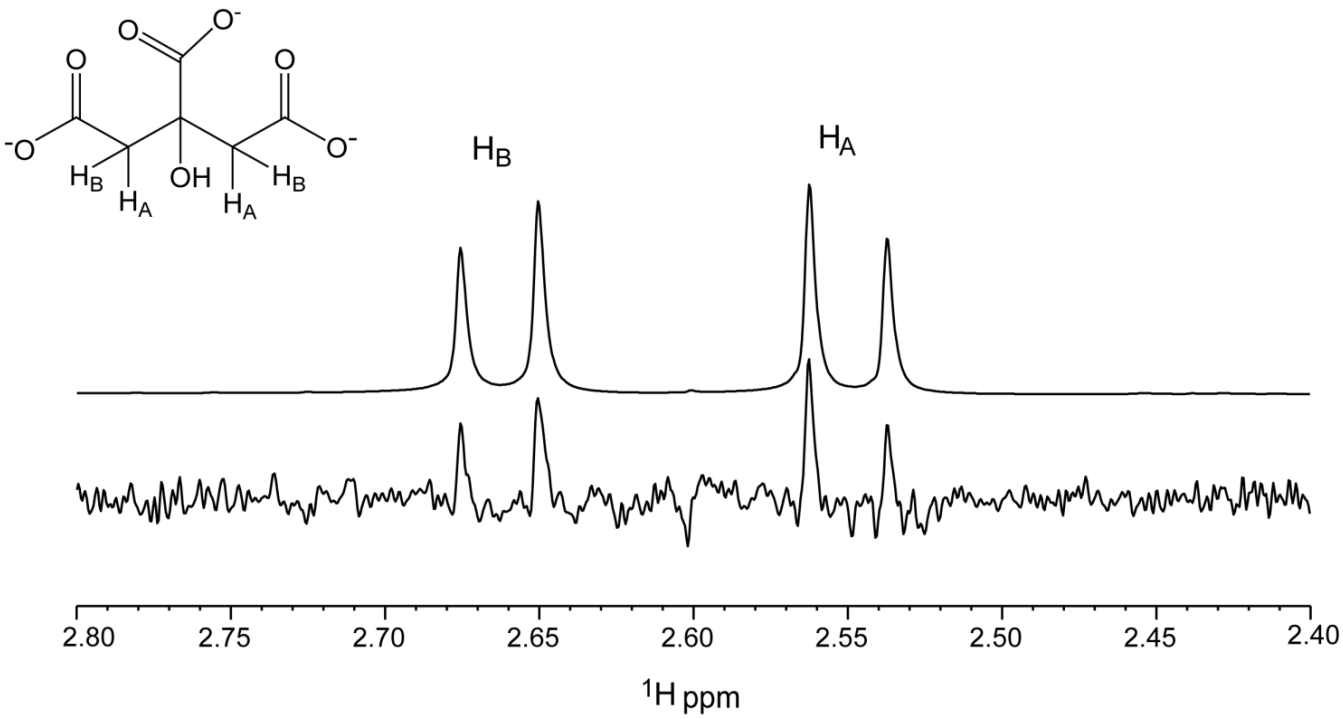

Figure S2. STD NMR spectra for citrate bound to GII.12 P domain. STD difference (lower) and reference (upper) spectra of citrate (2 mM) in the presence of GII.12 P domain (25 μM). Protons HA and HB of citrate show STD enhancements similar to those observed for binding to GII.10P domain, indicating a similar mode of binding and proximity to protein in the bound state.

Figure S3

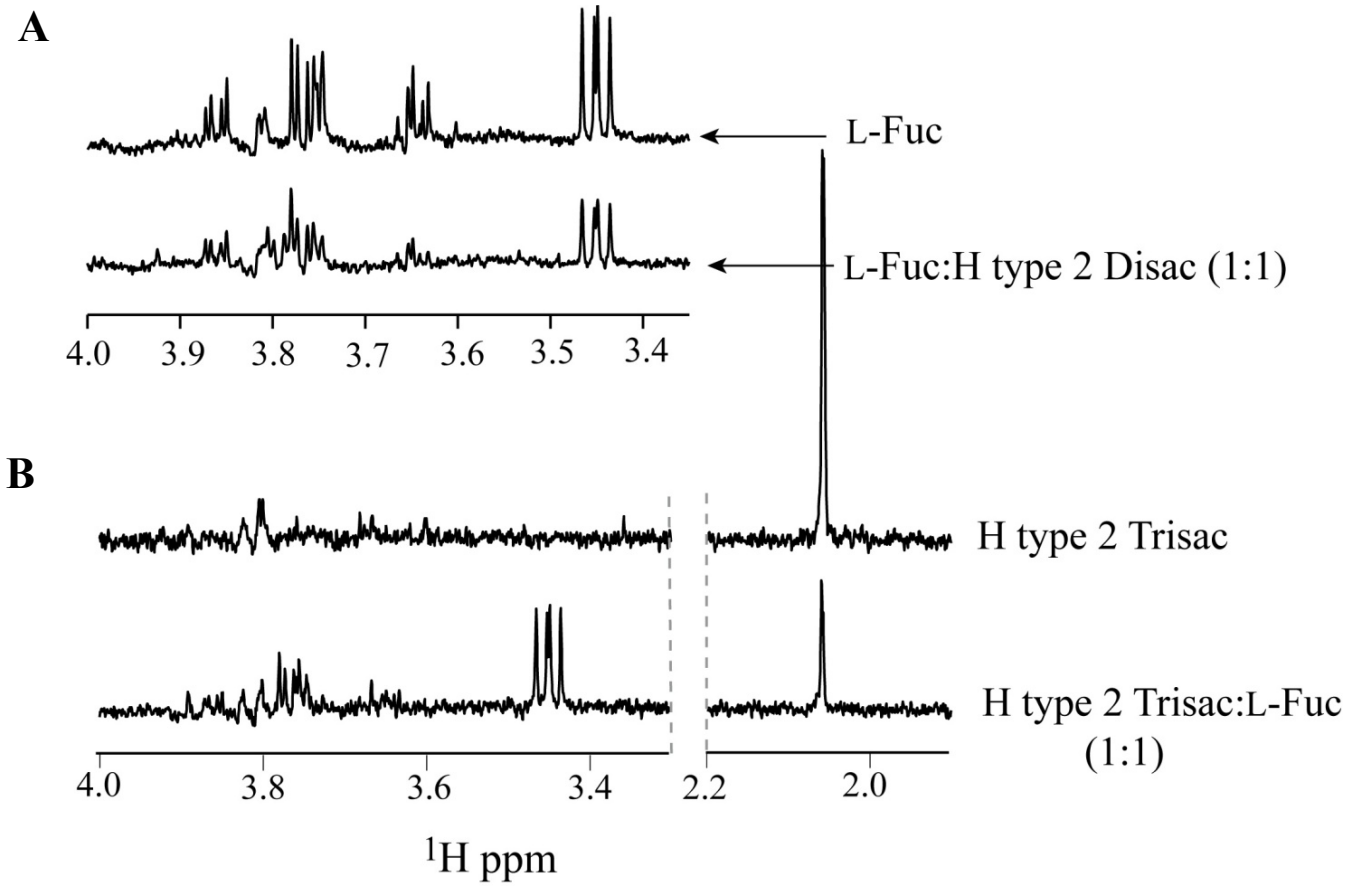

Figure S3. Competition STD NMR spectra for obtaining the K_D of L-fucose and H type 2 disaccharide. (A) STD NMR spectra of L-fucose (1.5 mM, upper), and 1:1 L-fucose:H type-2 disaccharide (1.5:1.5 mM, lower) used to obtain the K_D of H type-2 disaccharide. (B) STD spectra of H type-2 trisaccharide (1.5 mM, upper) and a 1:1 L-fucose:H type-2 trisaccharide (1.5:1.5 mM, lower) used to obtain the K_D of L-fucose binding to the GII.10 P domain.

Figure S4

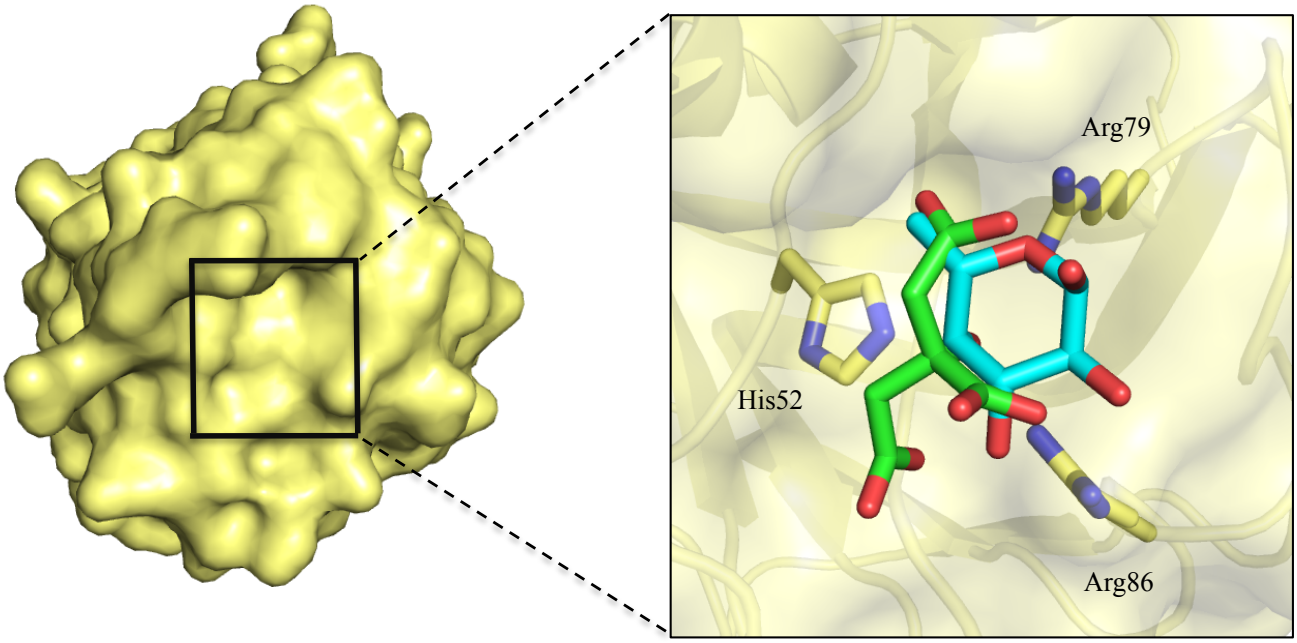

Figure S4. Computational citrate docking studies of *Anguilla anguilla* agglutinin *(PDB ID: 1K12).* The square bracket highlights the fucose binding site from the full protein surface. Docked citrate molecule is shown in green. The co-crystallized fucose is shown in cyan. The fucose molecule forms hydrogen bonds with the side chains of Arg86 (via O3), His52 (via O4), and Arg79 (via O5). The predicted citrate binding pose overlaps O5, C5, C4, O4, and C3 of fucose and forms hydrogen bonds with that same set of protein residues in a similar way as observed in the case for the GII.10 P domain.

Figure S5

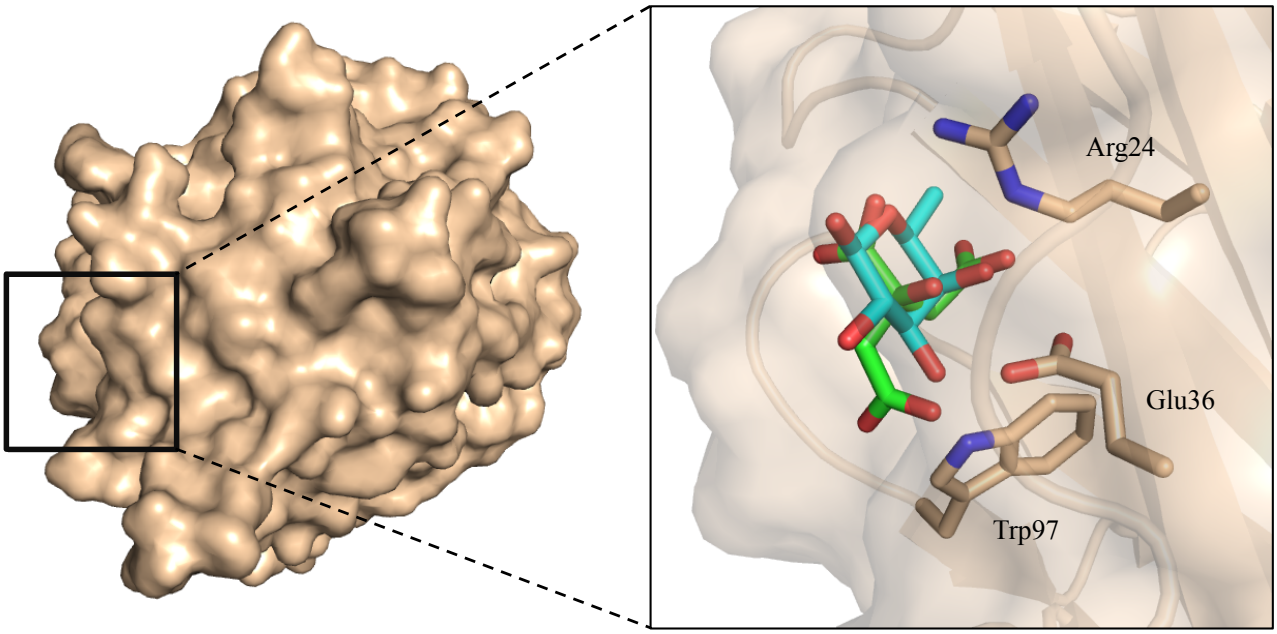

Figure S5. Computational citrate docking studies *of Aleuria aurantia* lectin (PDB ID: 1IUC). The square bracket highlights the fucose binding site from the full protein surface. Docked citrate molecule is shown in green. The fucose is shown in cyan. The co-crystallized fucose molecule forms hydrogen bonds with the side chains of Arg24, Glu36, and Trp97. The predicted citrate binding pose forms hydrogen bonds with that same set of protein residues.

Figure S6

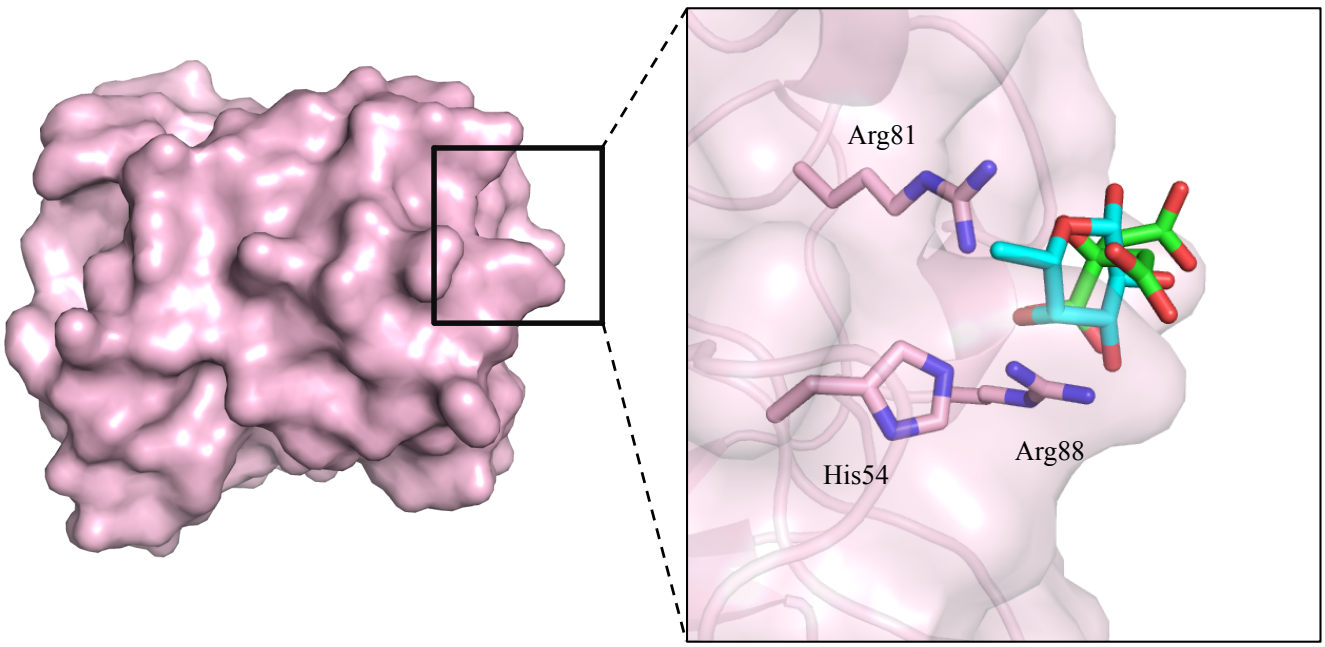

Figure S6. Computational citrate docking studies of *Streptococcus pneumoniae* virulence factor SpGH98 (PDB ID: 2J1S). The square bracket highlights the fucose binding site from the full protein surface. Docked citrate molecule is shown in green. The co-crystallized fucose is shown in cyan. The co-crystallized fucose molecule forms hydrogen bonds with the side chains of His54, Arg81, and Arg88. The predicted citrate binding pose forms hydrogen bonds with that same set of protein residues.

Figure S7

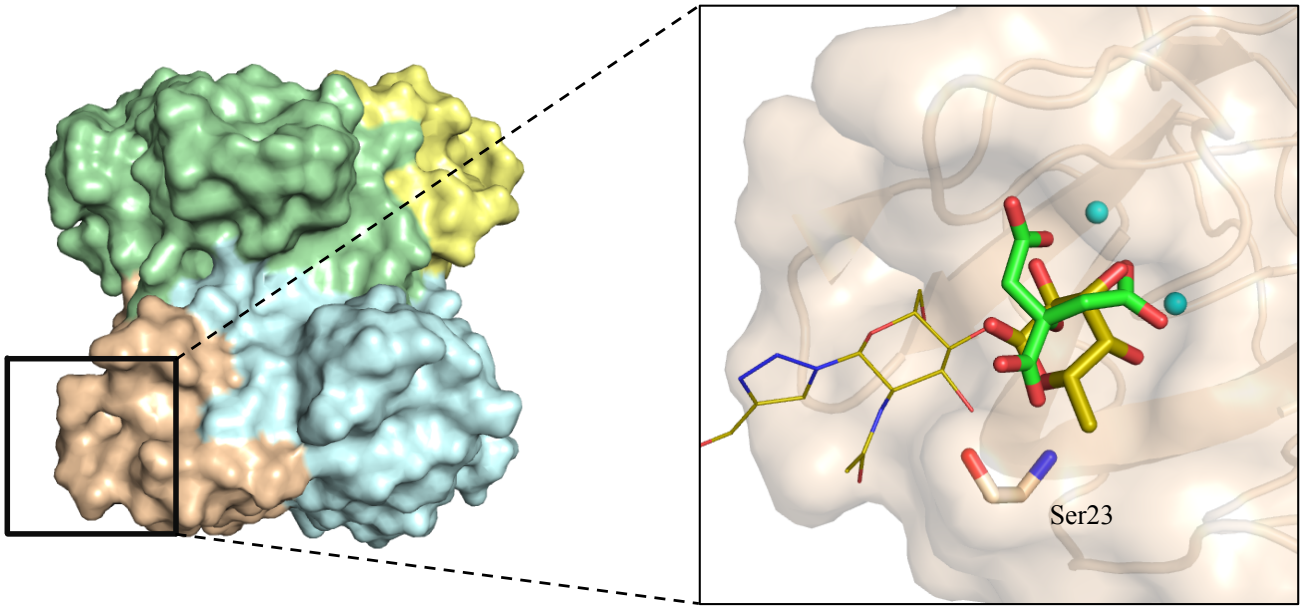

Figure S7. Computational citrate docking studies of *Pseudomonas aeruginosa* PA-IIL lectin (PDB ID: 2JDH). The square bracket highlights the inhibitor binding site from the full protein surface. Docked citrate molecule is shown in green. The co-crystallized disaccharide inhibitor is shown in gold, and the fucose moiety is shown as sticks. The fucose moiety forms hydrogen bonds with the main chain NH group of Ser23 and coordinates with two calcium ions (cyan spheres). The predicted citrate binding pose also forms hydrogen bonds with the main chain NH group of Ser23 and coordinates with the two calcium ions.

Figure S8

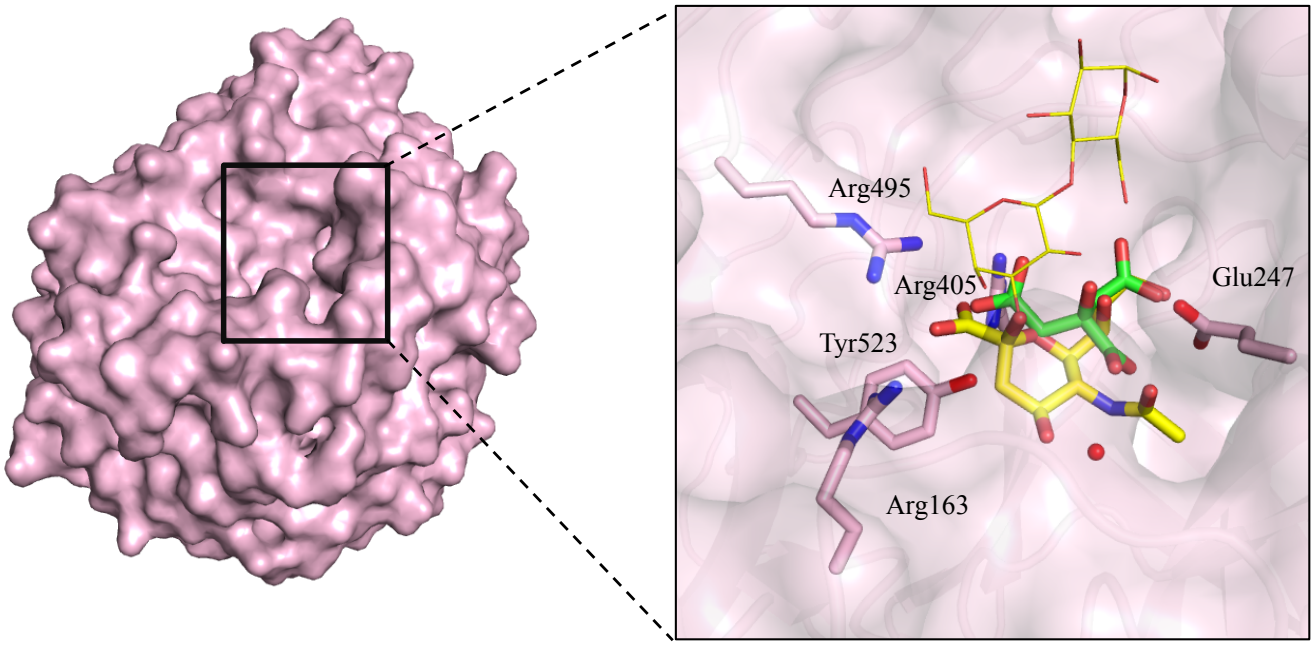

Figure S8. Computational citrate docking studies of parainfluenza virus 5 hemagglutinin-neuraminidase (PDB ID: 1Z4X). The square bracket highlights the sialyllactose binding site from the full protein surface. Docked citrate molecule is shown in green. The co-crystallized sialyllactose is shown in yellow, and the sialic acid moiety is shown as sticks. The sialic acid moiety forms hydrogen bonds with the side chains of Arg163, Arg405, Arg495, Tyr523, and Asp247, and also with a buried water molecule. The predicted citrate binding pose forms hydrogen bonds with the same set of protein residues and water molecule, with the exception of Arg163.

Figure S9

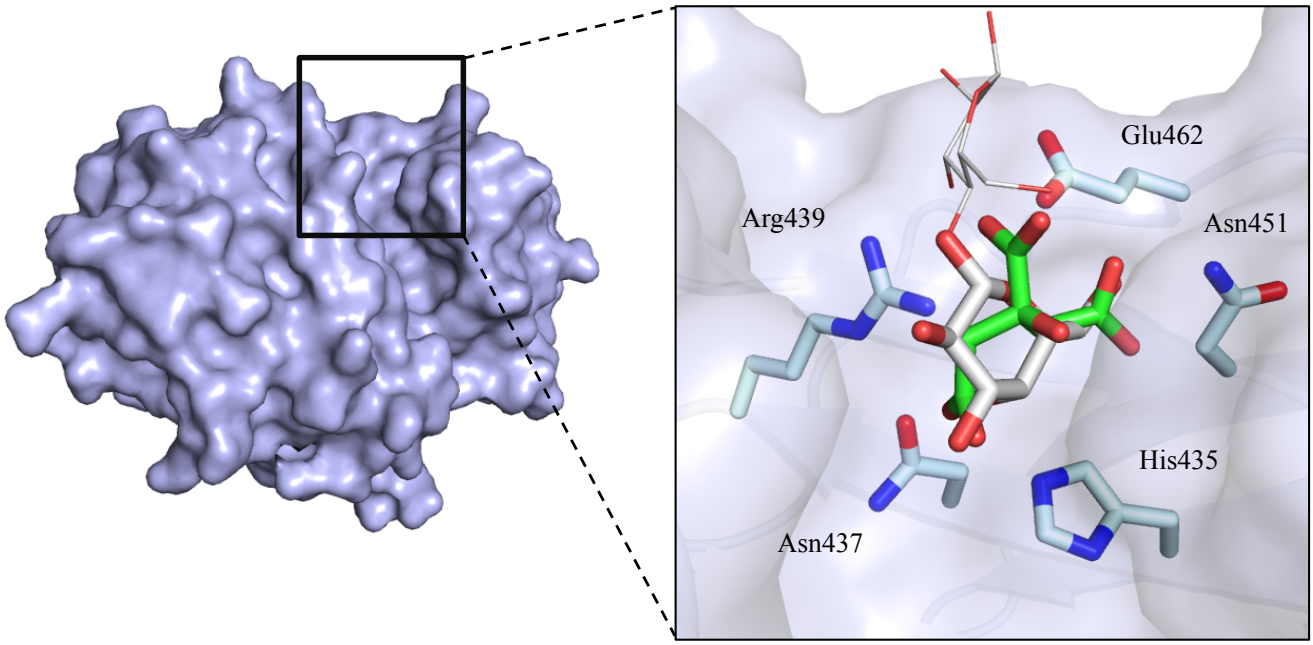

Figure S9. Computational citrate docking studies of porcine adenovirus type 4 galectin domain (PDB ID: 2WSV). The square bracket highlights the lactose binding site from the full protein surface. Docked citrate molecule is shown in green. The co-crystallized lactose is shown in silver, and the galactose moiety is shown as sticks. The galactose moiety forms hydrogen bonds with the side chains of Glu462, Asn451, His435, Asn437, and Arg439. The predicted citrate binding pose forms hydrogen bonds with that same set of protein residues.

Table S1. Docking results for citrate and monosaccharides against GII.10 P domain and six different saccharide-binding proteins using AutoDock4.2.

Protein		Co-crystallized	Monosaccharide Docking		Citrate Docking	Mimicry
PDB ID	Name	Monosaccharide[a]	Score (kcal/mol)	RMSD (Å)[b]	Score (kcal/mol)	RMSD (Å)[c]
3ONY	P domain	Fucose	-4.57	0.52	-4.27	0.67[d]
1K12	Agglutinin	Fucose	-3.62	1.15	-3.20	0.80
1IUC	Lectin	Fucose	-4.95	0.96	-4.11	2.72
2J1S	SpGH98	Fucose	-3.97	1.06	-2.56	2.67
2JDH	PA-IIL	Fucose	-5.03	0.88	-11.56	3.20
1Z4X	HN	Sialic acid	-6.24	2.91	-3.62	-
2WSV	Galectin domain	Galactose	-3.66	1.63	-3.77	-

[a]For non-monosaccharide ligands are the terminal monosaccharides having the largest contact area with the saccharide binding site.

[b]Root mean square deviation of the monosaccharide docking pose with respect to the co-crystallized monosaccharide.

[c]Root mean square deviation between six atom pairs from co-crystallized fucose and docked citrate: C5(fucose)-C2(citrate), C4(fucose)-C3(citrate), C3(fucose)-C3 COO(citrate), O5(fucose)-O C1OO(citrate), O4(fucose)-O C3O(citrate), and O3(fucose)-O C3COO(citrate).

[d]Co-crystallized citrate instead of docked citrate.